

Contents lists available at ScienceDirect

Renewable Energy

journal homepage: www.elsevier.com/locate/renene



Analytical solutions for predicting thermal plumes of groundwater heat pump systems



William Pophillat ^a, Guillaume Attard ^{a, *}, Peter Bayer ^b, Jozsef Hecht-Méndez ^c, Philipp Blum ^d

- ^a Cerema, Département Environnement Territoires Climat, 46 rue Saint-Théobald, F-38081 L'Isle d'Abeau, France
- b Ingolstadt University of Applied Sciences, Institute of new Energy Systems (InES), Esplanade 10, 85049 Ingolstadt, Germany
- ^c Amberg Engineering Technologies AG, Trockenloostrasse 21, Regensdorf, Switzerland
- d Karlsruhe Institute of Technology (KIT), Institute of Applied Geosciences (AGW), Kaiserstraße 12, 76131 Karlsruhe, Germany

ARTICLE INFO

Article history: Received 13 June 2018 Received in revised form 25 July 2018 Accepted 30 July 2018 Available online 4 August 2018

Keywords: Thermal impact Shallow geothermal energy Groundwater heat pump Numerical modelling Analytical solution Aquifer

ABSTRACT

Groundwater heat pump (GWHP) systems have gained attention for space heating and cooling due to their efficiency and low installation costs. Their number is growing in many countries, and therefore in some areas, dense installations are expected. This might lead to thermal interferences between neighbouring groundwater wells and a decrease in efficiency. In the presented study, three analytical formulations are inspected for the prediction of the thermal plume around such open-loop systems under various hydrogeological conditions. A thermal radial transport scenario without background groundwater flow and two advective scenarios with moderate to significant ambient flow velocities (1 and 10 m d⁻¹) are analytically simulated and compared with numerical simulations. Two-dimensional (2D) numerical models are used to estimate the validity of analytical results for a homogeneous confined aquifer, without considering heat transfer in upper and lower layers of the aquifer. In order to represent more realistic aquifer conditions of limited vertical extension, an additional three-dimensional numerical model (3D) is deployed to account for vertical heat losses. The estimated relative errors indicate that the analytical solution of the radial heat transport is in good agreement with both numerical model results. For the advective scenarios, the suitability of the linear and planar advective heat transport models strongly depend on ambient groundwater flow velocity and well injection rate. For low groundwater velocities ($1\,\mathrm{m}\,\mathrm{d}^{-1}$), the planar model fits both numerical model results better than the linear advective model. However, the planar model's ability to estimate thermal plumes considerably decreases for high injection rates (>0.6 l s⁻¹). In contrast, the linear advective model shows a good agreement with the twodimensional numerical results for high groundwater flow conditions ($\geq\!10\,m\,d^{-1}$). The comparison with the three-dimensional numerical models indicates that the vertical heat transfer is challenging for all of the selected analytical solutions. Despite this, there is a wide range of applicability for the provided analytical solutions in studying the thermal impact of GWHP systems. Hence, the inspected solutions prove to be useful candidates for first-tier impact assessment in crowded areas with potential thermal interferences.

© 2018 Elsevier Ltd. All rights reserved.

1. Introduction

Geothermal energy represents a large source of environmentally friendly energy with a potentially low carbon footprint [1,2]. The most common and versatile utilization of geothermal energy is direct use, and it is employed for a variety of applications such as

space heating, cooling, bathing, hot water and industrial uses [3]. These applications are mostly focused on using shallow geothermal resources at a shallow depth of not more than a few hundreds of meters [4,5]. Among the most frequently used variants are ground source heat pump (GSHP), ground water heat pump (GWHP) and aquifer thermal energy storage systems (ATES) (Fig. 1).

In GSHP systems, a closed-loop borehole heat exchanger (BHE) buried in the ground circulates a heat carrier fluid and is attached to a heat pump at the surface (Fig. 1a). GWHP systems (Fig. 1b), also

^{*} Corresponding author. E-mail address: guillaume.attard@cerema.fr (G. Attard).

Nomenclature table			Temperature difference between T and T_u [K]
		ΔT_o	Temperature difference at injection point [K]
A_T	Retarded velocity for radial flow [m s ⁻¹]	v_a	Seepage velocity [m s ⁻¹]
b	Thickness of aquifer [m]	X	x-coordinate [m]
C	Volumetric heat capacity [J $Kg^{-1} K^{-1}$]	y	y-coordinate [m]
D	Hydrodynamic dispersion [m ² s ⁻¹]	Y	Dimension of planar source in y-direction [m]
F_o	Energy injection per length of borehole [W m ⁻¹]	Y_0	Width of steady plume at injection well [m]
K	Hydraulic conductivity [m s ⁻¹]	Y_{max}	Maximum width of steady-state plume [m]
n	Porosity [-]	Z	z-coordinate [m]
q_h	Injected heat power [W]	α	Dispersivity [m]
Q_{inj}	Injection rate [m ³ s ⁻¹]	λ	thermal conductivity [W m^{-1} K ⁻¹]
r	Radial distance from injection well [m]	ho	Density [kg m ⁻³]
r*	Frontal position of heat plume [m]		
R	Retardation factor [—]	Subscrij	ots
t	Time [s]	w	Water
T	Calculated front temperature [K]	S	Soil
T_{inj}	Temperature of injected water [K]	m	Porous media
T_u	Undisturbed temperature of aquifer [K]	L	Longitudinal
ΔT_{inj}	Temperature difference between T_{inj} and T_u [K]	T	Transverse

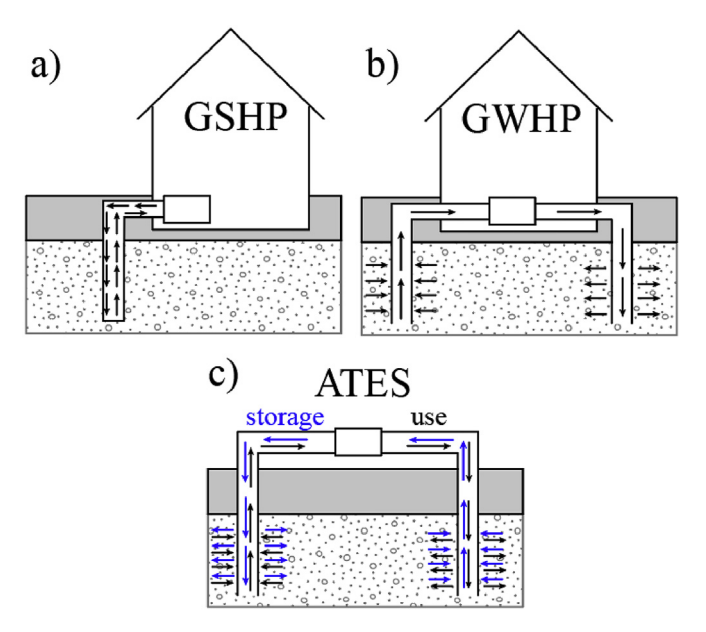


Fig. 1. Scheme of shallow geothermal systems: a) ground source heat pump (GSHP), b) ground water heat pump (GWHP) and c) aquifer thermal energy storage (ATES) systems.

known as open-loop systems [6–9], use groundwater extracted through a production well as a heat carrier fluid. In the heating mode, the groundwater mined at the temperature of the aquifer passes through a heat pump, where it exchanges heat and cools down before it is reinjected into the aquifer. As a result, a cold plume develops in the aquifer. In the cooling mode, the system is deployed in reverse mode. In this case, the aquifer is used as a sink of, for instance, waste heat and a thermal plume evolves in the aquifer. A special strategic application of open systems is the aquifer thermal energy storage (ATES) system (Fig. 1c). Similar to GWHP systems, water with a different temperature than the ambient groundwater temperature is injected and cooled/heated groundwater is extracted through wells [10,11]. The idea behind of ATES is to inject excess heat in an aquifer when it is available, store

it for a certain period and pump it back for heating, when it is needed.

Under favourable hydrogeological conditions such as high aquifer yield at shallow depth, suitable groundwater quality, etc., the use of GWHP systems is an attractive and efficient energy-saving option [12]. In addition, installation costs of GWHP systems are often lower than those of GSHP systems [13]. However, as the use of shallow geothermal energy is continuously growing, especially in urban areas, the numbers of GWHP installations increase and may reach a critical density [14–18]. This state is reached when adjacent GWHP installations show thermal interference with one another. For instance, if a new production well is installed in the thermal plume of an existing injection well, this could compromise the efficiency of the new system.

In order to account for case-specific hydrogeological and geothermal conditions, model-based site assessment and integrated planning is needed for optimal GWHP development in cities. Ambient groundwater flow yields elongated plumes, which deviate from the idealized circular shape, depending on natural groundwater flow direction, transient dynamics and aquifer heterogeneity. In this respect, several previous studies examined the thermal impact of heat or cold injection from GWHP and ATES systems. Among others, Andrews [19], Warner and Algan [20], Gropius [7], Nam and Ooka [21], García-Gil et al. [22], Russo et al. [23], Russo et al. [24] and Arola et al. [25] numerically simulated the effects of GWHP systems on the temperature distribution in aquifers. A common conclusion is that the thermal plume dimension around an operating well is site-specific and can critically affect neighbouring injection or production wells. Thus, GWHP systems are recommended to be installed in areas, where the interference can be avoided, or rigorous and proactive management of multiple adjacent GWHP systems is warranted. For example, Gropius [7] presented an evaluation of the risks associated with GWHP systems in the London Chalk aquifer, utilizing measured data, in addition to numerical flow and heat transport modelling. In their study, not only was the interaction between injection and extraction wells numerically assessed, but also the mutual impact between existing and planned neighbouring installations. The results corroborate the potential risk of thermal interference between adjacent GWHP systems.

Numerical models are considered the most appropriate method for simulating the thermal aquifer response to geothermal exploitation in shallow aquifers, especially in case of hydraulic heterogeneity, thermal variability and complex transient conditions [26–30]. Sophisticated urban planning concepts were presented for supporting geothermal development of shallow aquifers [15,18,31–33]. In practice, however, numerical models that sufficiently resolve the thermal and hydraulic conditions in aquifers are time-consuming and costly and therefore are not often available.

Alternatively, especially for an initial impact assessment of GWHP systems, simplified modelling procedures were suggested. For instance, Rauch [34] presented a two-dimensional (2D) estimation of the steady state temperature distribution around an injection well of a GWHP system based on the fluctuation angles of the groundwater flow streamlines. In his work, no formal analytical solution for the heat transport equation is used, but instead, the temperatures are calculated based on expected geometric features of the plume. The presented approach is only valid for scenarios with thin thermal plumes and it computes the plume length only up to the maximum thickness, and hence, the total length of the plume is not assessed. The procedure was used by Krakow and Fuchs-Hanusch [35] who assessed the potential user conflict of various planned GWHP systems in the city of Linz (Austria). Banks [36], and Galgaro and Cultrera [37] assess the risk of thermal feedback in open-loop double-well systems based on streamlinebased functions that, however, neglect thermal dispersion and diffusion. Comparison to numerical simulations that include these processes revealed that the streamline-based functions substantially overestimated the longitudinal extension of the thermal plume in its flow direction, as well as, in most cases, the transversal plume width [38]. A crucial aspect in this context is the definition of the thermal plume. It represents an area, where the temperature is sufficiently or critically altered. Most commonly, an isotherm is defined as a boundary [39] or arbitrary threshold of induced temperature difference such as 1 K [38–41]. Obviously, the smaller the threshold, the greater the thermal plume.

Analytical solutions of flow and heat transport equations are easy to use and therefore of growing interest for supporting licensing procedures. For instance, the "Guideline for the Use of Ground Water Heat Pumps Systems" from the state of Baden-Wuerttemberg, Germany [42], recommends an analytical solution for estimating thermal plume sizes caused by GWHP systems [43]. This analytical solution is deemed to serve as a regulatory tool for installation design, prospect and management of open-loop systems with an energy extraction of less than 45.000 kWh per year. However, since analytical solutions are developed for particular conditions; (e.g. one-, two- or three-dimensional, confined or unconfined, steady-state or transient, type of geometry of the source), special care has to be taken when using them in a broader sense or in another context. Thus, validity range of available and recommended analytical solutions are of high interest for supporting licensing or thermal impact studies of GWHP systems. Ideally, there exists one analytical solution that is sufficiently accurate for the variety of hydraulic and thermal conditions that can be found in the underground.

In the present study, the analytical approach used in the State of Baden-Wuerttemberg, as well as two other analytical solutions based on the line source and the planar source model are evaluated for heat transport simulations of GWHP systems. Predictions of the temperature distribution around an injection well in a homogeneous porous media under various hydraulic conditions are compared with more comprehensive numerical results. The key objective in this case is to specify the range of applicability of each analytical solution under various hydraulic conditions. This is accomplished by inspecting three scenarios that differ with respect to groundwater flow velocity, injection rate and thermal dispersion.

2. Materials and methods

2.1. Analytical solutions

The three studied analytical solutions, along with their main assumptions are listed in Table 1 and illustrated in Fig. 2. The first is a 2D solute transport analytical solution adapted for heat transport without natural groundwater flow (radial model) [42]. The other two consider effects of groundwater flow on heat transport (advective models). All of these analytical solutions do not account for vertical heat transport into the top and bottom of the aquifer and therefore they represent simplifications of the heat transport in porous media [44,45].

2.1.1. Radial heat transport model

Guimerà et al. [46] modified the 2D solute transport analytical solution given by Gelhar and Collins [47], which estimates the contaminant distribution in a homogeneous confined aquifer considering a fully penetrating injection well with no natural groundwater flow. This modified analytical solution for heat transport simulations and transient conditions, assuming a continuous line-source and no background groundwater flow reads as follows:

$$\frac{\Delta T(x, y, t)}{\Delta T_{inj}} = \frac{1}{2} \operatorname{erfc} \left\{ \frac{r^2 - r^{*2}}{2 \left[\left(\frac{4}{3} \alpha_L \right) (r^*)^3 + \left(\frac{\lambda m}{A_T C_m} \right) (r^*)^4 \right]^{1/2}} \right\}$$
(1)

with:

$$r^* = (2A_T t)^{\frac{1}{2}} \tag{2}$$

$$A_T = \left(\frac{nC_w}{C_m}\right) \left(\frac{Q_{inj}}{2\pi nb}\right) = \frac{1}{R} \left(\frac{Q_{inj}}{2\pi nb}\right)$$
(3)

 A_T denotes the retarded velocity caused by the injection rate Q_{inj} and r^* represents the frontal position of the heat plume. The frontal position is defined as the location of the hypothetical thermal front that would exist if dispersion and diffusion phenomena were neglected [47].

2.1.2. Linear advective heat transport model

The analytical solution, referred to as LAHM, is presented in the "Guideline for the Use of Ground Water Heat Pumps Systems" from the State of Baden Württemberg, Germany [48]. This 2D heat transport analytical solution was firstly introduced by Kinzelbach [49]. It describes heat propagation from an injection well with transient conditions, simulated as continuous line-source, considering background flow for a homogeneous confined aquifer. The LAHM reads as follows:

$$\Delta T(x, y, t) = \frac{Q_{inj} \ \Delta T_{inj}}{4nb\nu_a \sqrt{\pi\alpha_T}} \exp\left(\frac{x - r'}{2\alpha_L}\right) \ \frac{1}{\sqrt{r'}} \ \text{erfc} \left(\frac{r' - \nu_a t/R}{2\sqrt{\nu_a \alpha_L t/R}}\right)$$
(4)

with:

$$r' = \sqrt{x^2 + y^2 \frac{\alpha_L}{\alpha_T}} \tag{5}$$

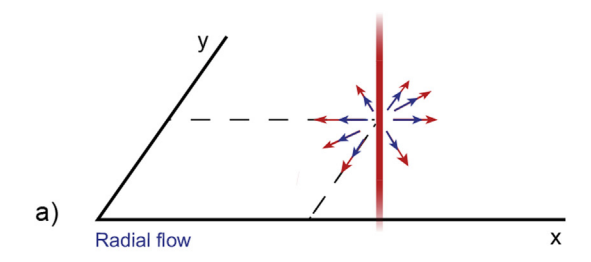
Dispersivity values (α_L and α_T) are estimated using a method that relies on the length of the plume [43].

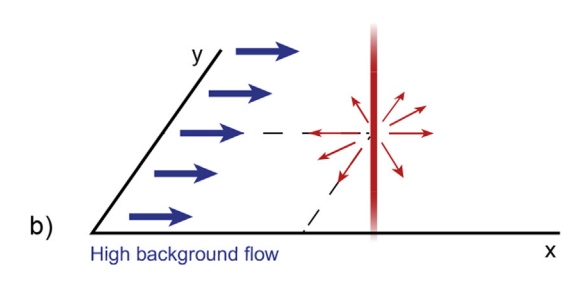
This analytical formulation is an approximation of the exact solution for uniform background flow. It does neither consider

 Table 1

 Analytical solutions used for the simulation of open systems.

Analytical solution	Abbreviation	Assumptions
Radial heat transport model Linear advective heat transport model Planar advective heat transport model	RHM LAHM PAHM	2D, transient, line source, continuous injection, radial transport from injection well, no background flow. 2D, transient, line source, continuous injection, background flow. 2D, transient, planar source, continuous injection, background flow.





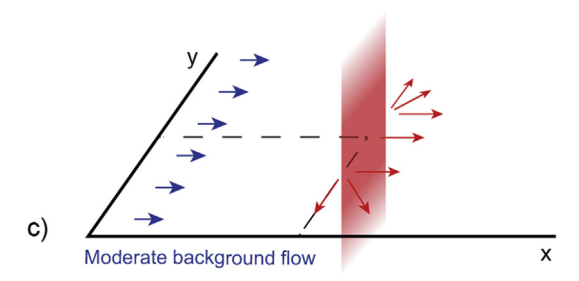


Fig. 2. Scheme of the analytical models considered. a) Radial heat transport model. b) Linear advective heat transport model. c) Planar advective heat transport model.

conduction in the aquifer nor the hydraulic influence of the injected water in the vicinity of the well [43]. According to this guideline, its applicability is constrained to low injection rates, at an energy use lower than 45,000 kWh per year and of groundwater flow velocities higher than 1 m d $^{-1}$. Moreover, for $r'/(2\alpha_L)>1$, this solution leads to less than 10% error in comparison with the exact solution. For $r'/(2\alpha_L)>10$, the error reduces to less than 1% [49].

2.1.3. Planar advective heat transport model

Due to the limited application window of the LAHM, an alternative analytical solution is evaluated for intermediate cases, i.e. cases in between low and high groundwater flow (1 and 10 m d^{-1}). The planar advective heat transport model (PAHM) accounts for the fact that injection may induce a high local hydraulic gradient around the injection well. In such a case, the geometry of this heat source cannot be considered only with a vertical line. Instead, the source is represented as an area in the *yz*-plane. Accordingly, in a 2D horizontal projection in the *xy*-plane, the heat source corresponds to a line perpendicular to the groundwater flow direction.

The PAHM was introduced by Domenico and Robbins [50], as a 2D solute transport analytical solution for transient conditions and homogeneous parallel groundwater flow, assuming a continuous

and finite planar source. The transformed equation for heat transport is described in Hähnlein et al. [51]. Note that this solution was developed for a semi-infinite domain, and therefore it ignores the zone up-gradient from the source location:

$$\Delta T(x, y, t) = \left(\frac{\Delta T_0}{4}\right) \operatorname{erfc}\left(\frac{Rx - v_a t}{2\sqrt{D_x Rt}}\right) \left\{\operatorname{erf}\left[\frac{y + \frac{Y}{2}}{2\sqrt{D_y \frac{X}{v_a}}}\right] - \operatorname{erf}\left[\frac{y - \frac{Y}{2}}{2\sqrt{D_y \frac{X}{v_a}}}\right]\right\}$$
(6)

 ΔT_0 is the temperature difference in the injection point and is given by:

$$\Delta T_0 = \frac{F_0}{\nu_a n C_W Y} \tag{7}$$

with

$$F_0 = \frac{q_h}{h} \tag{8}$$

$$q_h = \Delta T_{inj} C_w Q_{inj} \tag{9}$$

where F_0 is the energy injection per length of the borehole (W m⁻¹), Y is the dimension of the source in the y-direction and q_h is the injected heat power. The parameters D_x and D_y in Equation (6) are the longitudinal and transversal hydrodynamic dispersion coefficients, respectively, and they are defined as follows:

$$D_{x,y} = \frac{\lambda_m}{nC_{xx}} + \alpha_{L,T} \nu_a \tag{10}$$

The subscripts L and T refer to longitudinal and transversal direction with respect to the groundwater flow direction.

Two formulations are compared to determine the source length Y:

$$Y_0 = \frac{Q_{inj}}{2bv_a n} \tag{11}$$

$$Y_{max} = \frac{Q_{inj}}{bv_a n} \tag{12}$$

Equation (11) quantifies the width, Y_0 , of the steady plume at the injection well, and Equation (12) computes the maximum (downgradient) width, Y_{max} , of the steady-state plume [52]. The planar heat model associated with Equations (11) and (12) is referred to as PAHM1 or PAHM2, respectively.

2.2. Numerical simulation

Numerical modelling is performed to assess the applicability of the analytical solutions in various scenarios. To start, 2D numerical models are used to estimate the validity of analytical results for a homogeneous confined aquifer, without considering vertical heat

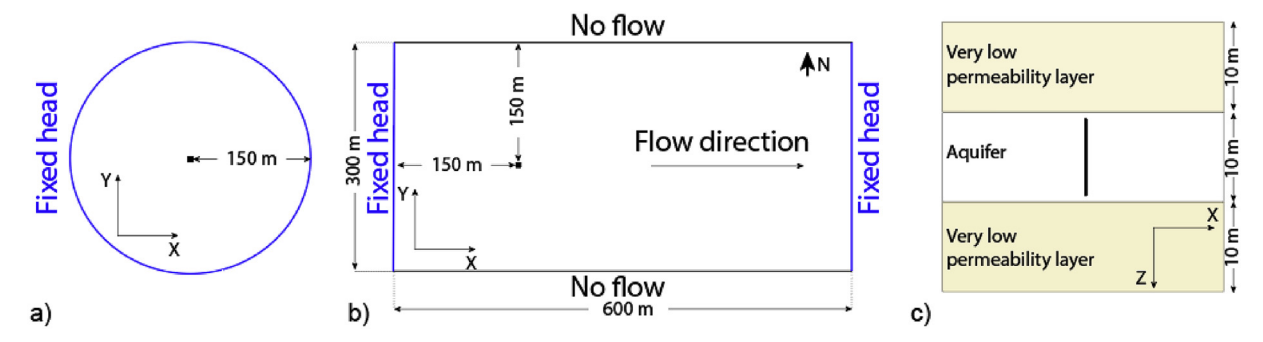


Fig. 3. Model geometry and flow boundary conditions. Black squares (a and b) and rectangle (c) represent the injection well. (a) Schematic top view of the radial model (2D and 3D). (b) Schematic top view of advective models (2D and 3D). (c) Schematic cross section of the 3D models.

transfer into upper and lower layers. This model set-up is chosen to be consistent with the conceptual assumptions of the 2D analytical models, and to represent conditions with substantial aquifer widths, where the relative contribution of vertical heat exchange is low and thus negligible. Then, a three-dimensional (3D) model with vertical heat flux is used to evaluate the consequences of this simplified assumption. The modelling process consists of solving transient heat transport and flow equations for the entire studied area. Groundwater flow and heat transport are simulated using FEFLOW [53]. This software is based on the finite element method and was applied for heat transport in related studies [23,31,39,54,55].

Given that the thermal stress in the subsurface is highest during peak summer conditions [56], we evaluated the thermal impact by using a GWHP system injection well in cooling mode. This is the scenario when warm water is injected into the aquifer through the injection well. The conceptual model assumes that the aquifer is confined, saturated, homogeneous and of a constant thickness within the entire domain. Water is continuously injected at constant rate and temperature into the aquifer through a fully penetrating well. Fluid density, viscosity and thermal parameters of the aquifer (specific heat capacity and thermal conductivity) are assumed to be constant [4]. The ambient temperature of the aquifer is initially constant (285.15 K) and the only internal source of energy is the well. No temporal variations and no recharge are considered. Heat transport simulations are performed for 120 days of continuous injection.

The configuration used in 2D numerical models is illustrated in Fig. 3a and b. Only the injection well (represented by a black point) is simulated, assuming that the production well is far away from it and that no hydraulic interference occurs. For the radial model, the domain covers a circle of 150 m radius (Fig. 3a), in order to respect the cylindrical symmetry of the simulated problem. In the advective model, the domain is a rectangle of 600 m by 300 m (Fig. 3b). A horizontal mesh is applied using a triangular algorithm. The size of the elements ranges from several centimetres near the injection well to about a meter near to the domain boundaries.

The configuration used in the 3D numerical models is illustrated in Fig. 3c. The aquifer (10 m thick, horizontal) is located between two layers with low-permeability (10 m thick, horizontal). The horizontal geometry is identical to that of the 2D models (Fig. 3a and b). The 3D models span $600~\text{m}\times300~\text{m}\times30~\text{m}$ for the advective scenarios and a cylinder of 150~m radius and 30~m thickness for the radial scenario. Vertical discretization is accomplished by 22 horizontal layers with a refinement in the aquifer and is close to the interfaces between the aquifer and the low-permeability layers. The size of the horizontal elements ranges from several centimetres at a position near the injection well to about 3~m at the model boundaries. In the 3D model, the vertical geometry of the injection

well is represented by a vertical series of seven nodes located from 10.5 m to 19.5 m depth (Fig. 3c).

For the radial model, the same hydraulic Dirichlet boundary condition (BC) is assigned to the entire boundary (Fig. 3a). For the advective models, Dirichlet BCs are specified at the west and east boundaries, resulting in a new forced flow from west to east (Fig. 3b). Recharge at the injection well is simulated by assigning nodal source BCs to the well node. Warm water injection is simulated in two different ways. By default, the convective form of the heat transport equation [57] is solved and the temperature injection is represented by defining Dirichlet BCs (constant temperature) at well nodes. Therefore, the injected water has the temperature imposed by the Dirichlet BCs. However, the imposed temperature at the well nodes adds an additional input of energy by conduction. It leads to overestimating the actual heat flux injected by an amount that depends on the thermal gradient in the vicinity of the well nodes [58]. When the overestimation of the total stored heat energy exceeds 5%, the simulation is restarted by assigning constant heat nodal source BCs to well nodes and by using the divergent form of the heat transport equation [57]. This second solution enables control over the total heat flux, except for the temperature at the well location. The final configurations used for comparisons to analytical simulations are listed in Table 2.

Three different scenarios are created based on their corresponding groundwater flow velocities (Table 2, Fig. 4a). The scenarios are defined based on typical hydraulic conductivity values of three hydrogeological units: very fine sand, coarse sand and fine gravel [59] for scenarios 1, 2 and 3, respectively, in which all keep a constant hydraulic gradient of 5×10^{-3} (except for scenario 1, where it is zero). Scenario 1 represents a model without natural background flow ($v_a = 0 \text{ m d}^{-1}$) while scenarios 2 ($v_a = 1 \text{ m d}^{-1}$) and 3 ($v_a = 10 \text{ m d}^{-1}$) represent moderate and strongly advection-dominated cases, respectively.

In addition, three model variants are defined (Fig. 4b) based on three different volumetric flow rates, different dispersity values and a different set of predefined temperature changes ($\Delta T = 10 \, \text{K}$). The resulting estimated energy loads are in a good agreement with energy requirements of a typical residential use (e.g. one family or multi-family house [20]). Table 2 shows the hydraulic, hydrogeological and thermal input parameters entered in the flow and heat transport code as well as in the analytical solutions.

2.3. Comparison method between analytical and numerical results

The ability of analytical solutions to predict the temperature field for the three scenarios and their variants is evaluated by comparing the estimates they provide with results from numerical modelling. A first step in each scenario is to compare analytical results with 2D numerical results. This comparison aims to evaluate

Table 2 Parameter values for the analytical and numerical models (Var. = variant).

	Scenario 1	Scenario 2	Scenario 3		
Fluxes					
$v_a ({\rm m} {\rm d}^{-1})$	0	1	10		
Q_{inj} (1 s ⁻¹)	Var. 1: 2	Var. 1: 2	Var. 1: 2		
	Var. 2: 0.6	Var. 2: 0.6	Var. 2: 0.6		
	Var. 3: 0.3	Var. 3: 0.3	Var. 3: 0.3		
q_h (J s ⁻¹)	Var. 1: 8.37×10^4	Var. 1: 8.37 × 10 ⁴	Var. 1: 8.37×10^4		
	Var. 2: 2.51×10^4	Var. 2: 2.51 × 10 ⁴	Var. 2: 2.51×10^4		
	Var. 3: 1.26×10^4	Var. 3: 1.26×10^4	Var. 3: 1.26×10^4		
Material properties					
Aquifer (2D, 3D)					
b (m)	10	10	10		
n (-)	0.3	0.3	0.3		
K (m s ⁻¹)	10 ⁻⁵	6.94×10^{-4}	6.94×10^{-3}		
$\alpha_L(m)^a$	1	1.8	Var. 1: 6.2		
<u>L</u> ()			Var. 2: 1.8		
			Var. 3: 1.0		
$\alpha_T(\mathbf{m})^{\mathbf{a}}$	0.1	0.18	Var. 1: 0.62		
<i>u</i> ₁ (III)	0.1	0.10	Var. 2: 0.18		
			Var. 3: 0.10		
Upper and lower layers (3D)		var. 5. 0.10		
b (m)	10	10	10		
n (-)	0.3	0.3	0.3		
$K \text{ (m s}^{-1})$	10 ⁻⁹	10 ⁻⁹	10 ⁻⁹		
$\alpha_L(\mathbf{m})^a$	1	1	1		
$\alpha_T(\mathbf{m})^{\mathbf{a}}$	0.1	0.1	0.1		
Thermal properties	0.1	0.1	0.1		
$T_u(K)$	285.15	285.15	285.15		
$T_{ini}(K)$	295.15	295.15	295.15		
$\lambda_w (W \text{ m}^{-1} \text{ K}^{-1})$	0.578	0.578	0.578		
λ_s (W m ⁻¹ K ⁻¹)	4	4	4		
$\lambda_m (W \text{ m}^{-1} \text{ K}^{-1})^b$	2.24	2.24	2.24		
C_w (J m ⁻³ K ⁻¹)	4.185×10^{6}	4.185×10^{6}	4.185×10^{6}		
$C_s (J m^{-3} K^{-1})$	4.185×10^{6} 2.332×10^{6}	$\frac{4.185 \times 10}{2.332 \times 10^6}$	4.185×10^{6} 2.332×10^{6}		
$C_m (J m^{-3} K^{-1})$	2.332×10^{6} 2.888×10^{6}	2.332×10 2.888×10^{6}	$2.332 \times 10^{\circ}$ 2.888×10^{6}		
Boundary conditions	2.000 × 10	2,000 × 10°	2,000 × 10		
Domain	Fixed head	Fixed head on west and east boundaries	Fixed head on west and east boundaries		
Well (flow)	Nodal source	Nodal source	Nodal source		
Well (heat)	Fixed temperature	Var. 1 and 2: fixed temperature Var. 3: nodal source	Nodal source		

^a Calculated after Umweltministerium Baden-Württemberg [48] and Keim & Lang [43].

the consistency of analytical results with those obtained from simplified numerical models that similarly neglect vertical heat transport. In a second step, analytical results are compared with the predictions from 3D models that also simulate the influence of heat transfer in the upper and lower layers. This second comparison aims thereby to evaluate the capability of the analytical solutions to reproduce more realistic conditions with aquifers of limited vertical extension.

For each case, the evaluation focuses on the analytical models' ability to estimate the local temperatures $(T_{\rm xy})$ and the extension of the area where the thermal impact exceeds 1 K (hereafter 1 K-plume). For the 1 K-plumes extension, two parameters are considered: the length (L) of the 1 K-plume and its maximal width (W). Note that since the PAHM does not allow to calculate the temperature field up-gradient from the injection well, for scenario 2 $(v_a = 1 \text{ m d}^{-1})$ the length and the width are calculated only for the part of the plume located down-gradient from the well.

Analytical estimates of these three parameters are evaluated by calculating the relative errors (RE) between analytical and numerical results according to Equation (13) (by considering the numerical results as reference values).

$$XRE = 100 \cdot \frac{X_{analytic} - X_{numeric}}{X_{numeric}}\%$$
 (13)

Where *X* denotes the considered parameter (L, R or T_{xy}). The relative error can be positive or negative, reflecting respectively an analytical overestimation or underestimation of the considered parameter. When |XRE| < 10%, the analytical estimate of the parameter is considered good. When 10% < |XRE| < 30%, it is considered satisfactory. When 30% < |XRE| < 50%, it is weak. When |XRE| > 50%, the analytical result is considered improper.

3. Results

Comparative simulation results are presented in Table 3, Figs. 5 and 6. Table 3 lists the derived relative errors of the 1 K-plumes extensions after 120 days of continuous injection. Fig. 5 depicts the 2D view of the plumes. Fig. 6 shows the relative error between analytical and 3D numerical estimates of the local temperature, calculated at any point on the domain. For further information, Figure A1 (Appendix) presents the distribution of the energy injected between storage in the aquifer, storage in the upper and lower layers and transfers outside of the domain.

3.1. Scenario 1: radial flow

In scenario 1, no ambient groundwater flow is considered ($v_a = 0 \text{ m d}^{-1}$) and the RHM analytical solution is compared with numerical results. Because of the radial flow symmetry, plume

^b Calculated after Johansen [60] and Woodside & Messmer [61].

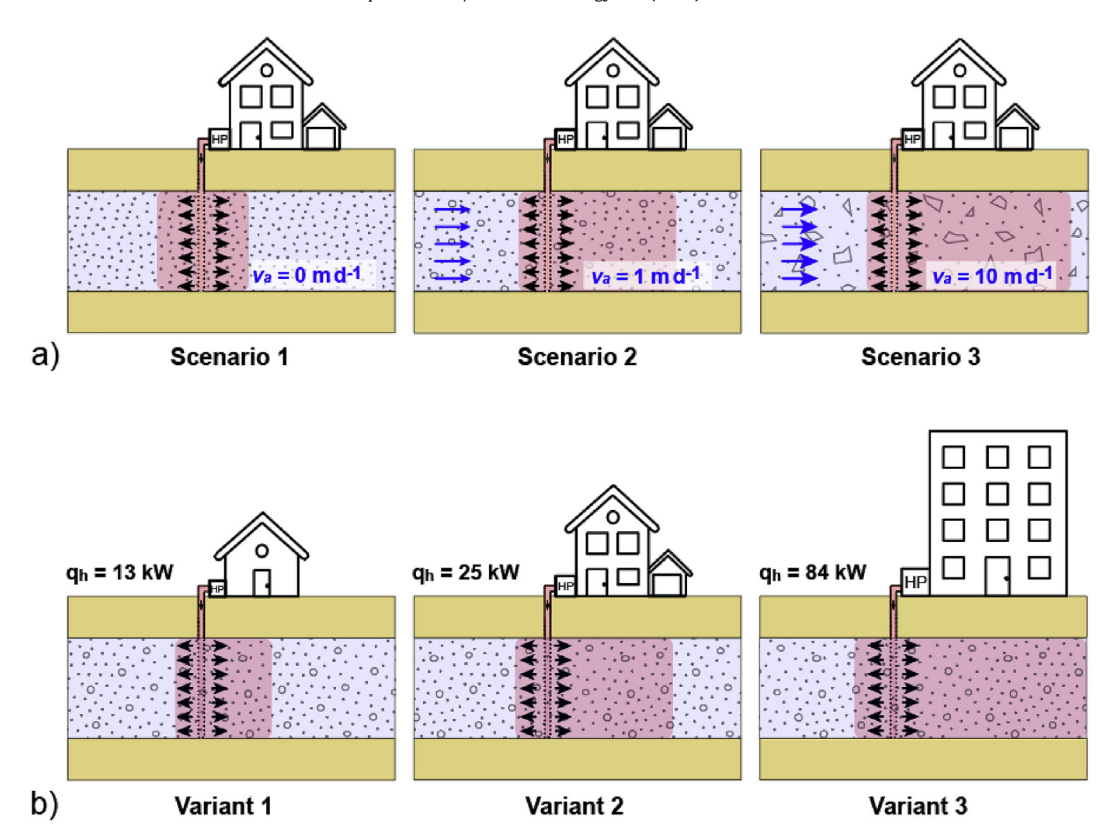


Fig. 4. Scheme of the three scenarios (a) and variants presented for scenario 2 (b).

Table 3Relative error between analytical and numerical estimates of the length (LRE) and the maximal width (WRE) of the zones where the thermal impact exceeds 1 K. LRE and WRE are given in percentages.

Scenario	Variant	Model	2D comparison		3D comparison	
			LRE	WRE	LRE	WRE
$v_a = 0 \text{ m d}^{-1}$	$Q_{inj} = 2.0 l s^{-1}$	RHM	-1	-1	3	3
	$Q_{inj} = 0.6 \mathrm{l s^{-1}}$	RHM	-3	-3	2	2
	$Q_{ini} = 0.3 l s^{-1}$	RHM	-3	-3	1	1
$v_a = 1 \text{ m d}^{-1}$	$Q_{inj} = 2.0 \mathrm{l s^{-1}}$	LAHM	-9	-65	-2	-63
	,	PAHM1	-14	-25	-7	-21
		PAHM2	-20	16	-13	23
	$Q_{inj} = 0.6 l s^{-1}$	LAHM	-4	-44	5	-39
	,	PAHM1	-7	-19	2	-13
		PAHM2	-9	-4	0	4
	$Q_{inj} = 0.3 1 s^{-1}$	LAHM	-1	-32	11	-25
		PAHM1	-4	-10	7	-2
		PAHM2	-5	-6	7	3
$v_a = 10 \text{ m d}^{-1}$	$Q_{inj} = 2.0 l s^{-1}$	LAHM	4	1	65	12
	$Q_{ini} = 0.6 l s^{-1}$	LAHM	16	0	36	1
	$Q_{inj} = 0.3 \mathrm{l s^{-1}}$	LAHM	26	0	26	-8

length and width are equal. We thus only refer to the LRE.

In this scenario, the analytical and 2D numerical results agree well for the three variants (Table 3). There is only a minor increase of LRE as the injection rate decreases. This confirms that when the vertical heat transport can be neglected, RHM provides good estimates of the 1 K-plumes' dimensions.

When comparing this with the findings from a 3D numerical simulation of vertical heat transfer, it reveals that the differences are only marginal (Fig. 5 and A1 in Appendix). RHM estimates of the 1 K-plume extension thus remain good when taking into account the vertical heat transport. In this case, RHM estimates of the local temperature are also good, except in a small radial area where the

T_{xv} RE slightly exceeds 10% (Fig. 6).

3.2. Scenario 2: moderate background flow

In scenario 2, a moderate seepage velocity is considered ($v_a = 1 \text{ m d}^{-1}$), and therefore the analytical solutions PAHM (1 and 2) and LAHM are compared with numerical results. Note that the seepage velocity value for this scenario is the lowest allowed for using the LAHM model by the guideline mentioned in section 2.1.2 [48].

For the three variants, the LAHM simulation is, for the most part, closest to the 2D numerical simulation of the 1 K-plumes' length. In addition, this is the only analytical solution that is able to describe the thermal impact up-gradient of the injection well. However, this model predicts elongated plume shapes and underestimates the width of the 1 K-plume. This discrepancy is especially pronounced for high injection rates. The PAHM (1 and 2) assume a planar source. Consequently, the simulated plume widths are closer to the numerical results than those by the LAHM. Still, PAHM1 predicts plume widths that are up to 25% smaller than 2D-numerical calculations for high injection rates ($Q_{inj} = 21 \,\mathrm{s}^{-1}$). PAHM2 assumes a greater transversal source size and thus estimated plume widths are greater than those by the PAHM1. Especially for conditions with high injection rates, the predicted plumes are too sizeable. However, even if the source width appears inappropriate for the simulated plumes (see Fig. 5), comparison of maximum 1 K-plume width between PAHM2 and numerical 2D simulation reveals overall satisfactory results. Additionally, if the 1 K-plume lengths predicted by the PAHM simulations are less appropriate than those by the LAHM for 2D conditions, they remain overall satisfactory. Therefore, for hydrogeological conditions similar to those considered here, the PAHM2 is favourable for predicting the 1 K-plume extension.

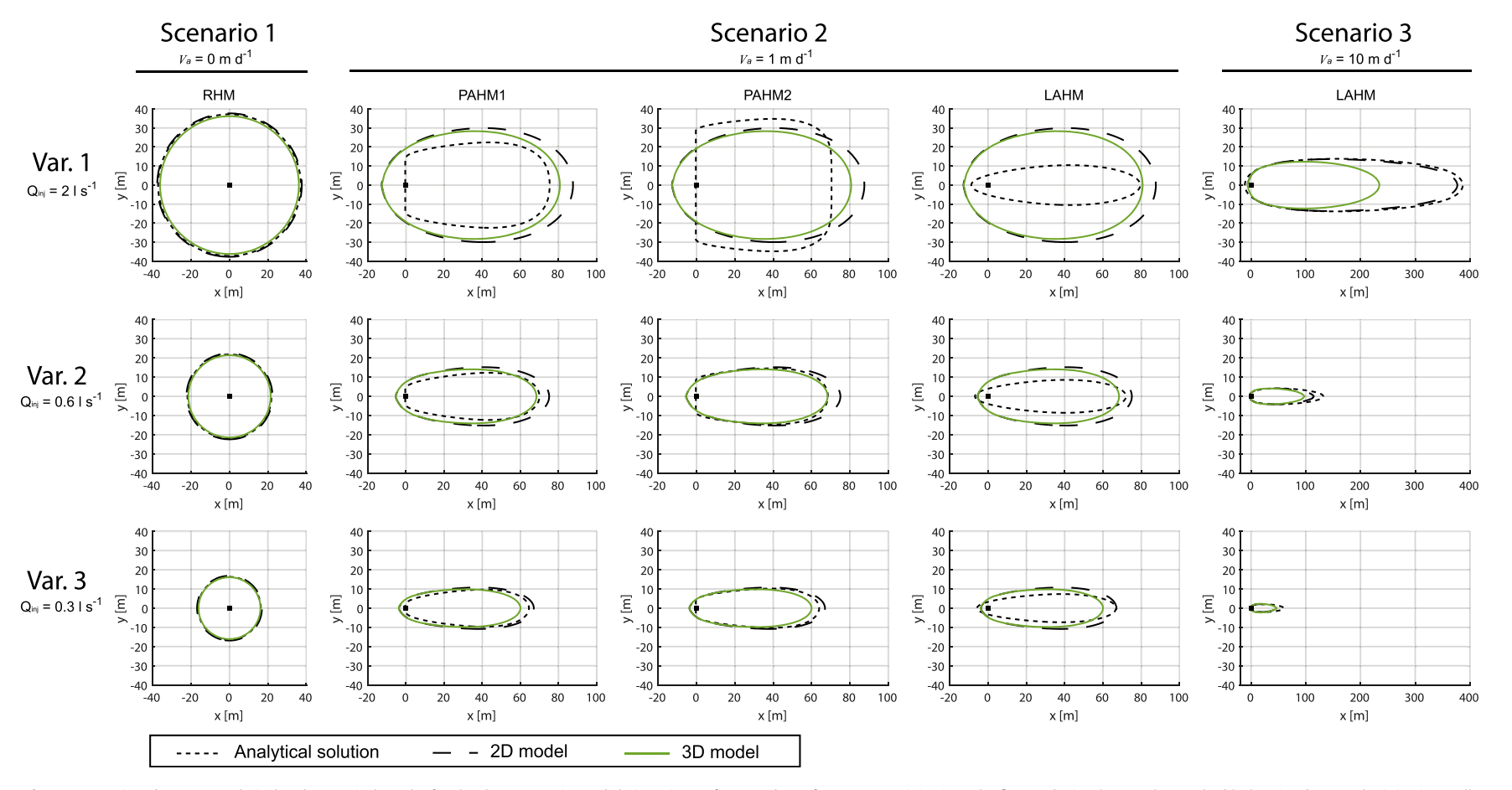


Fig. 5. Comparison between analytical and numerical results for the three scenarios and their variants after 120 days of warm water injection. The figures depict the 1 K-plume. The black point denotes the injection well.

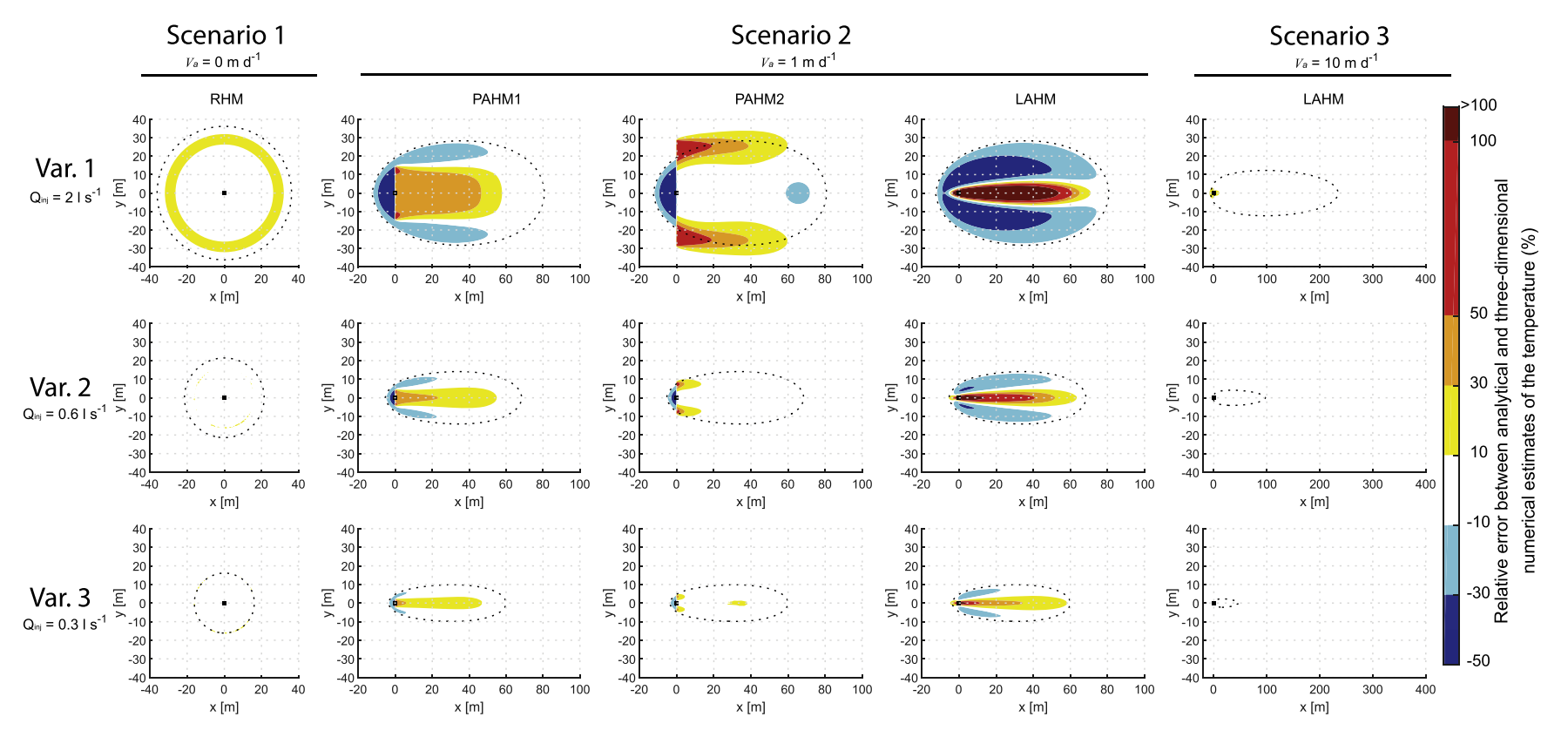


Fig. 6. Spatial distribution of local relative error (in %) between analytical and 3D numerical results. In addition, 1 K-plumes calculated by the 3D numerical model are shown. Areas where the absolute value of the relative error is less than 10% are depicted in white.

Comparison with 3D numerical results demonstrates that heat loss in the top and bottom of the aquifer is higher than in the radial scenario, and it rises with the well injection rate. However, the extensions of the plumes do not significantly change (Fig. 5). The agreement between analytical and 3D numerical estimates of the 1 K-plume extension thus remains similar to that of the 2D numerical results. Fig. 6 confirms the previous findings and it shows, in addition, that PAHM provides better estimates of the local temperatures than LAHM for all variants.

The omission of the vertical heat transport in the analytical models does not yield a significant overestimation. With or without considering vertical heat transport, LAHM and PAHM are both suitable for approximating the 1 K-plume length. However, the PAHM is superior when the width of the plume has to be estimated. PAHM2 provides overall better results than PAHM1. For moderate injected rates ($Q_{inj} \leq 0.6 \, \mathrm{l \, s^{-1}}$), it can be applied for reliable prediction of the 1 K-plume extension and satisfactory estimates of the local temperature. Still, the accuracy decreases near to the well and this solution cannot describe thermal impact up-gradient from the well. For high injection rates, PAHM2 simulations of the 1 K-plume extension remain satisfactory.

3.3. Scenario 3: high background flow

Scenario 3 assumes a very high groundwater flow velocity of $v_a = 10 \, \mathrm{m \, d^{-1}}$. Such conditions are not within the recommended validity range of the PAHM and thus focus is set on the LAHM. The comparison between analytical and 2D numerical results shows that LAHM slightly overestimates the 1 K-plume length (Table 3, Fig. 5). While a good approximation of the 1 K-plumes length is found for $Q_{inj} = 2.01 \, \mathrm{s^{-1}}$, it becomes weaker as the injection rate decreases. For the three variants, the 1 K-plumes width is well estimated by LAHM. This comparison with a numerical model close to the conceptual assumptions of the LAHM confirms that when the vertical heat transport can be neglected, LAHM well estimates the 1 K-plume dimensions.

A comparison with 3D numerical results in Fig. 5 reveals the high influence of heat transfer in upper and lower layers on the computed plumes' lengths, especially for $Q_{inj} = 2.01 \text{ s}^{-1}$. Figure A1, which depicts the relative distribution of injected heat after the simulated period, confirms this observation. More than 33% of the heat is lost in vertical direction for this scenario, whereas in the previous cases, this value has not reached above 30%. It is a given that high groundwater flow velocity expands the contact area between aquifer and adjacent layers, as it increases the ratio between plume area and volume and thus promotes vertical heat loss. For $Q_{inj} = 2.01 \,\mathrm{s}^{-1}$, this leads to an analytical overestimation of the 1 Kplume length by 65%. This error decreases with the injection rate and when the LRE for $Q_{inj} = 0.3 \, \mathrm{l \, s^{-1}}$ equals that of the 2D model. Vertical heat transfer seems to have less influence on the 1 K-plume width and LAHM offers satisfactory results. Additionally, as depicted in Fig. 6, the spatially distributed relative error between analytical and 3D numerical results remains overall less than 10% (except of near to the injection well), regardless of the injection rate. Thus, even if LAHM overestimates the 1 K-plumes length, its ability to estimate the local temperature (except of that near to the well) is very good. This reflects the strong spreading of the thermal anomaly induced by heat injection and high groundwater flow velocity. Even if local temperatures can be well reproduced by the analytical approach, the small thermal gradients make it difficult to properly delineate isotherms.

4. Discussion

The suitability of the three analytical solutions was examined

under various hydraulic conditions in homogeneous aquifers. For most of the tested conditions, there is an analytical solution able to assess 1 K-plume dimensions to a reasonable degree. This result offers great perspectives for integrated spatial planning in the case of dense geothermal use in cities, to avoid interferences between neighbouring wells. However, the comparison between analytical and 3D numerical results showed that even if analytical solutions can suitably estimate the thermal plume dimensions, they are not always appropriate to quantify local thermal impacts, for example near to the injection well. In these cases, analytical solutions should not be used for other purposes than to estimate plume dimensions, i.e. thermal impact assessment related to environment or technical consequences. Furthermore, an analytical model might well predict the temperature distribution at high ambient groundwater flow conditions, the strong plume spreading however hampers a reliable delineation of the 1 K plume. This, however, reflects that a broad zone exists under such conditions, where induced temperature changes are close to 1 K.

Finally, some crucial assumptions had to be made in order to assess the validity of these analytical solutions. In particular, the role of transient dynamics and sequential seasonal operation were not investigated in the presented work. Hence, attention has to be paid to these when analytical solutions are used to assess the impact of GWHP systems with variable discharges. In fact, Lo Russo et al. [23], used a deterministic model to simulate the influence of time discretization of the temporal variation of a GWHP operation in Torino (Italy). They showed that their simulations, based on seasonally mean values, are not satisfactory to describe the thermal impact of the GWHP system in operation. Also, the effect of heterogeneous hydraulic parameters, as well as of variable thermodynamic parameters such as dispersivity, thermal conductivity and heat capacity on the thermal plume development, may differ among specific cases [37,38], and their role should be scrutinized in further studies.

5. Conclusions

Groundwater heat pump (GWHP) systems generate thermal impacts, which in crowded areas are likely to affect the efficiency of neighbouring installations. In order to facilitate integrated and spatial underground management of such open geothermal systems, legal regulations and guidelines on these systems in the present, or in the future, require fast and efficient methods to evaluate thermal impact. In the present study, the suitability of three analytical solutions for 2D predictions of the thermal impact are therefore examined under various hydrogeological and flow conditions.

Our results show that the thermal impact on a homogeneous aquifer without natural background flow can be well estimated by the radial transport solution (RHM), given by Gelhar and Collins [47] and Guimerà et al. [46]. For the studied conditions, including an omission of the vertical heat transport does not result in a significant overestimation of the thermal impact.

The thermal impact of warm water injected with a low rate $(Q_{inj} \leq 0.61 \, \text{s}^{-1})$ in an aquifer with moderate groundwater natural flow velocity $(1 \, \text{m d}^{-1})$ can be estimated by the downgradient of the injection well by using a planar source model (PAHM) with satisfaction. The linear source model (LAHM) is suited for predicting the length of the 1 K-plume, but is not recommended for simulating the transversal width of the thermal plume. With increasing injection rates, discrepancies between analytical and numerical models occur, reflecting that the hydraulic impact of the well on the flow regime is not well reproduced by the presented analytical solutions.

When the ambient groundwater flow velocity is high

 $(\ge 10~{\rm m~d}^{-1})$, the linear source model is the only and best choice for approximating the thermal plume dimensions, especially for high injection rates and negligible vertical heat loss. There is, however, no appropriate model for prediction of exact plume lengths under these highly dynamic conditions, resulting in an overestimation of the thermal impact.

The presented study offers a comparison of available analytical solutions, which are straightforward to use and therefore of interest for the thermal impact assessment of GWHP systems. In addition, these analytical solutions can be used for supporting integrated spatial planning in case of dense geothermal use in cities. They are not intended to replace numerical simulations but to constitute a complementary tool in order to improve the management of the groundwater and geothermal resources. Despite the range of the different conditions analysed, suitable application ranges of the three analytical models for rough estimation of expected plume widths and lengths prove to be broad. This clearly depends on the threshold of acceptable prediction discrepancies. These are considered marginal when the relative error is smaller than 10%. These could be even tolerable when the relative error is below 30% for a first-tier assessment, as other uncertainties such as heterogeneity and groundwater flow direction are still present. Of course, the appropriate threshold has to be ultimately decided for each specific case.

Acknowledgements

We thank Nelson Molina-Giraldo for his assistance in the analytical simulations and Enzio Schoffer for language editing. This work was supported by the German Research Foundation (project number BA2850/3-1) and by the French Ministry of Ecological and Solidarity Transition.

Appendix

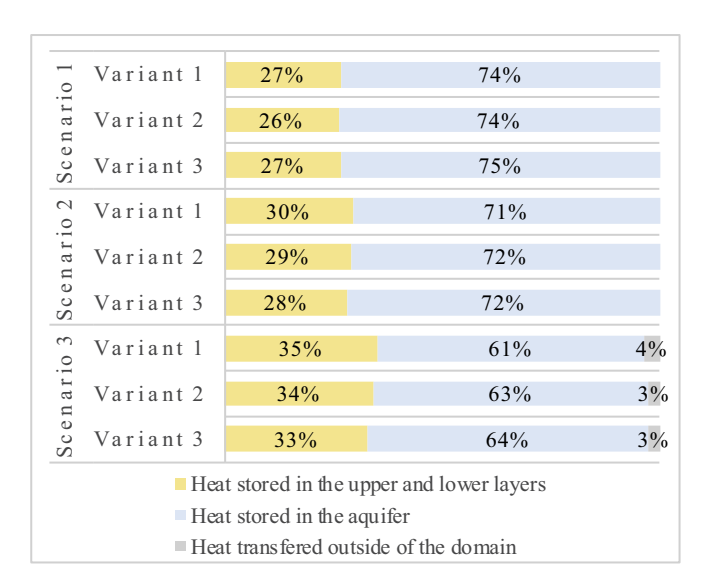


Fig. A1. Repartitioning of the energy injected between storage in the aquifer, storage in upper and lower layers and transfer outside of the model domain.

References

- [1] P. Blum, G. Campillo, W. Münch, T. Kölbel, CO₂ savings of ground source heat pump systems a regional analysis, Renew. Energy 35 (1) (2010) 122–127.
- [2] D. Saner, R. Juraske, M. Kübert, P. Blum, S. Hellweg, P. Bayer, Is it only CO₂ that matters? A life cycle perspective on shallow geothermal systems, Renew.

- Sustain. Energy Rev. 14 (7) (2010) 1798-1813.
- [3] J.W. Lund, T.L. Boyd, Direct utilization of geothermal energy 2015 worldwide review, Geothermics 60 (2016) 66–93.
- [4] J. Hecht-Méndez, N. Molina-Giraldo, P. Blum, P. Bayer, Evaluating MT3DMS for heat transport simulation of closed geothermal systems, Ground Water 48 (5) (2010) 741–756.
- [5] L. Rybach, Geothermal energy: sustainability and the environment, Geothermics 32 (4-6) (2003) 463-470.
- [6] F. De Keuleneer, P. Renard, Can shallow open-loop hydrothermal well-doublets help remediate seawater intrusion? Hydrogeol. J. 23 (4) (2015) 619–629.
- [7] M. Gropius, Numerical groundwater flow and heat transport modelling of open-loop ground source heat systems in the London Chalk, Q. J. Eng. Geol. Hydrogeol. 43 (1) (2010) 23–32.
- [8] V.L. Freedman, S.R. Waichler, R.D. Mackley, J.A. Horner, Assessing the thermal environmental impacts of an groundwater heat pump in southeastern Washington State. Geothermics 42 (2012) 65–77.
- Washington State, Geothermics 42 (2012) 65–77.

 [9] X. Zhou, Q. Gao, X. Chen, M. Yu, X. Zhao, Numerically simulating the thermal behaviors in groundwater wells of groundwater heat pump, Energy 61 (2013) 240–247.
- [10] M. Bloemendal, T. Olsthoorn, F. Boons, How to achieve optimal and sustainable use of the subsurface for aquifer thermal energy storage, Energy Pol. 66 (2014) 104–114.
- [11] M. Bloemendal, N. Hartog, Analysis of the impact of storage conditions on the thermal recovery efficiency of low-temperature ATES systems, Geothermics 71 (2018) 306–319
- [12] K. Rafferty, Well-pumping issues in commercial groundwater heat pump systems. Build. Eng. 104 (1998).
- [13] K.D. Rafferty, Commercial open loop heat pump systems, ASHRAE J. March (2009) 52–62.
- [14] S. Hähnlein, P. Bayer, G. Ferguson, P. Blum, Sustainability and policy for the thermal use of shallow geothermal energy, Energy Pol. 59 (2013) 914–925.
- [15] S.M. Maya, A. García-Gil, E.G. Schneider, M.M. Moreno, J. Epting, E. Vázquez-Suñé, M.Á. Marazuela, J.Á. Sánchez-Navarro, An upscaling procedure for the optimal implementation of open-loop geothermal energy systems into hydrogeological models, J. Hydrol. 563 (2018) 155–166.
- [16] J. Epting, F. Händel, P. Huggenberger, Thermal management of an unconsolidated shallow urban groundwater body, Hydrol. Earth Syst. Sci. 17 (2013) 1851–1869.
- [17] G. Ferguson, Unfinished business in geothermal energy, Ground Water 47 (2) (2009) 167.
- [18] A. Herbert, S. Arthur, G. Chillingworth, Thermal modelling of large scale exploitation of ground source energy in urban aquifers as a resource management tool, Appl. Energy 109 (2013) 94–103.
- [19] C. Andrews, The impact of the use of heat pumps on ground-water temperatures, Ground Water 16 (6) (1978) 437–443.
- [20] D. Warner, U. Algan, Thermal impact of residential ground-water heat pumps, Ground Water 22 (1) (1984) 6–12.
- [21] Y. Nam, R. Ooka, Numerical simulation of ground heat and water transfer for groundwater heat pump system based on real-scale experiment, Energy Build. 42 (1) (2010) 69–75.
- [22] A. García-Gil, E. Vázquez-Suñe, E.G. Schneider, J.Á. Sánchez-Navarro, J. Mateo-Lázaro, The thermal consequences of river-level variations in an urban groundwater body highly affected by groundwater heat pumps, Sci. Total Environ. 485 (2014) 575–587.
- [23] S.L. Russo, L. Gnavi, E. Roccia, G. Taddia, V. Verda, Groundwater Heat Pump (GWHP) system modeling and Thermal Affected Zone (TAZ) prediction reliability: influence of temporal variations in flow discharge and injection temperature, Geothermics 51 (2014) 103–112.
- [24] S.L. Russo, G. Taddia, E.C. Abdin, V. Verda, Effects of different re-injection systems on the thermal affected zone (TAZ) modelling for open-loop groundwater heat pumps (GWHPs), Environ. Earth Sci. 75 (1) (2016) 48.
- [25] T. Arola, J. Okkonen, J. Jokisalo, Groundwater utilisation for energy production in the Nordic environment: an energy simulation and hydrogeological modelling approach, J. Water Resour. Protect. 8 (06) (2016) 642.
- [26] A. García-Gil, E. Vázquez-Suñe, E.G. Schneider, J.Á. Sánchez-Navarro, J. Mateo-Lázaro, Relaxation factor for geothermal use development—Criteria for a more fair and sustainable geothermal use of shallow energy resources, Geothermics 56 (2015) 128—137.
- [27] K. Zhu, P. Bayer, P. Grathwohl, P. Blum, Groundwater temperature evolution in the subsurface urban heat island of Cologne, Germany, Hydrol. Process. 29 (6) (2015) 965–978.
- [28] J.W. Molson, E.O. Frind, Thermal Energy Storage in an unconfined aquifer 2. Model development, validation and application, Water Resour. Res. 28 (10) (1992) 2857–2867.
- [29] A. Casasso, R. Sethi, Modelling thermal recycling occurring in groundwater heat pumps (GWHPs), Renew. Energy 77 (2015) 86–93.
- [30] B.-H. Park, S.-W. Ha, K.-K. Lee, Minimum Well Separation for Small Groundwater Heat Pump (GWHP) Systems in Korea: Preliminary Analysis Based on Regional Aquifer Properties, 2017.
- [31] J. Epting, A. García-Gil, P. Huggenberger, E. Vázquez-Suñe, M.H. Mueller, Development of concepts for the management of thermal resources in urban areas—Assessment of transferability from the Basel (Switzerland) and Zaragoza (Spain) case studies, J. Hydrol. 548 (2017) 697–715.
- [32] M.H. Mueller, P. Huggenberger, J. Epting, Combining monitoring and

- modelling tools as a basis for city-scale concepts for a sustainable thermal management of urban groundwater resources, Sci. Total Environ. 627 (2018) 1121–1136.
- [33] J. Liang, Q. Yang, L. Liu, X. Li, Modeling and performance evaluation of shallow ground water heat pumps in Beijing plain, China, Energy Build. 43 (11) (2011) 3131–3138.
- [34] W. Rauch, Ausbreitung von Temperaturanomalien im Grundwasser, Universität Innsbruck, Innsbruck, 1992.
- [35] S. Krakow, D. Fuchs-Hanusch, Fernkälteversorgung zur Vermeidung von Grundwassererwärmungen und Nutzungskonflikten am Beispiel der Stadt Linz—Bewertung auf Basis ÖWAV-Regelblatt 207 und qualitativer NutzwertanalyseDistrict cooling to avoid groundwater warming and user conflicts using the example of the city Linz—Evaluation with ÖWAV-norm 207 and qualitative efficiency analysis, Österreichische Wasser-und Abfallwirtschaft 68 (7—8) (2016) 354—367.
- [36] D. Banks, The application of analytical solutions to the thermal plume from a well doublet ground source heating or cooling scheme, Q. J. Eng. Geol. Hydrogeol. 44 (2) (2011) 191–197.
- [37] A. Galgaro, M. Cultrera, Thermal short circuit on groundwater heat pump, Appl. Therm. Eng. 57 (1–2) (2013) 107–115.
- [38] B. Piga, A. Casasso, A. Godio, R. Sethi, Thermal impact assesment of ground-water heat pumps (GWHPs): rigorous vs. Simplified models, Energies 10 (2017) 1385.
- [39] S.L. Russo, G. Taddia, V. Verda, Development of the thermally affected zone (TAZ) around a groundwater heat pump (GWHP) system: a sensitivity analysis, Geothermics 43 (2012) 66–74.
- [40] N. Molina-Giraldo, P. Bayer, P. Blum, Evaluating the influence of thermal dispersion on temperature plumes from geothermal systems using analytical solutions, Int. J. Therm. Sci. 50 (7) (2011) 1223–1231.
- [41] N. Molina-Giraldo, P. Blum, K. Zhu, P. Bayer, Z. Fang, A moving finite line source model to simulate borehole heat exchangers with groundwater advection, Int. J. Therm. Sci. 50 (12) (2011) 2506–2513.
- [42] Umweltministerium Baden-Württemberg, Leitfaden zur Nutzung von Erdwärme mit Grundwasserwärmepumpen, in: U. Baden-Württemberg (Ed.), 2009. Stuttgart.
- [43] B. Keim, U. Lang, Nutzung der Erdwärme mit Grundwasserwärmepumpen, Umweltministerium Baden-Württemberg, Stuttgart, 2008.
- [44] F. Stauffer, P. Bayer, P. Blum, N.M. Giraldo, W. Kinzelbach, Thermal use of Shallow Groundwater, CRC Press, 2013.
- [45] Y. Shaw-Yang, Y. Hund-Der, An analytical solution for modeling thermal energy transfer in a confined aquifer system, Hydrogeol. J. 16 (8) (2008)

- 1507-1515.
- [46] J. Guimerà, F. Ortuño, E. Ruiz, A. Delos, A. Pérez-Paricio, Influence of Groundsource Heat Pump on Groundwater, European Geothermal Congress, Germany, 2007.
- [47] L.W. Gelhar, M.A. Collins, General analysis of longitudinal dispersion in nonuniform flow, Water Resour. Res. 7 (6) (1971).
- [48] Umweltministerium Baden-Württemberg, Arbeitshilfe zum Leitfaden zur Nutzung von Erdwärme mit Grundwasserwärmepumpen, in: U. Baden-Würrtemberg (Ed.), 2009, Stuttgart.
- [49] W. Kinzelbach, Numerische Methoden zur Modellierung des Transports von Schadstoffen im Grundwasser, 2 ed., Oldenbourg, München, 1987.
- [50] P. Domenico, G. Robbins, A new method of contaminant plume analysis, Ground Water 23 (4) (1985).
- [51] S. Hähnlein, N. Molina-Giraldo, P. Blum, P. Bayer, P. Grathwohl, Ausbreitung von Kältefahnen im Grundwasser bei Erdwärmesonden, Grundwasser 15 (2) (2010) 123–133.
- [52] H. Kobus, H. Mehlhorn, Temperaturefelder im Grundwasser, in: l.f.U. baden-Württemberg (Ed.), 1980.
- [53] H.-J.G. Diersch, FEFLOW: Finite Element Modeling of Flow, Mass and Heat Transport in Porous and Fractured Media, Springer Science & Business Media, 2013.
- [54] G. Attard, Y. Rossier, T. Winiarski, L. Eisenlohr, Deterministic modeling of the impact of underground structures on urban groundwater temperature, Sci. Total Environ, 572 (2016) 986–994.
- [55] V. Wagner, P. Bayer, M. Kübert, P. Blum, Numerical sensitivity study of thermal response tests, Renew. Energy 41 (2012) 245–253.
- [56] S. Lo Russo, M.V. Civita, Open-loop groundwater heat pumps development for large buildings: a case study, Geothermics 38 (3) (2009) 335–345.
- [57] H. Diersch, About the Difference between the Convective Form and the Divergence Form of the Transport Equation in FEFLOW White Papers, vol. I, DHI-WASY GmbH, Berlin, Germany, 2007.
- [58] S. Dupasquier, Contribution à l'étude du comportement thermo-hydraulique du stockage saisonnier de chaleur en aquifère, Thèse, Ecole polytechnique de Lausanne, 2000.
- [59] K. Spitz, J. Moreno, A Practical Guide to Groundwater and Solute Transport Modelling, John Wiley & Sons, United States of America, 1996.
- [60] O. Johansen, Thermal conductivity of Soils, Cold Regions Research and Engineering Lab Hanover NH, 1977.
- [61] W. Woodside, J. Messmer, Thermal conductivity of porous media. I. Unconsolidated sands, J. Appl. Phys. 32 (9) (1961) 1688–1699.